Bacteriorhodopsin as an electronic conduction medium for biomolecular electronics

Yongdong Jin,*[a] Tal Honig,[ab] Izhar Ron,[ab] Noga Friedman,[a] Mordechai Sheves*[a] and David Cahen*[b]

Received 5th June 2008
First published as an Advance Article on the web 19th September 2008
DOI: 10.1039/b806298f

Interfacing functional proteins with solid supports for device applications is a promising route to possible applications in bio-electronics, -sensors, and -optics. Various possible applications of bacteriorhodopsin (bR) have been explored and reviewed since the discovery of bR. This *tutorial review* discusses bR as a medium for biomolecular optoelectronics, emphasizing ways in which it can be interfaced, especially as a thin film, solid-state current-carrying electronic element.

1. Introduction

In biomolecular electronics (BME), native as well as modified biological molecules (chromophores, functional proteins, *etc*.) are studied as possible active elements in electronic and optoelectronic devices. A major driving force to study BME is the idea that biological molecules are optimized for given tasks by evolution and natural selection and that some of these tasks may be of interest for optoelectronic devices. In addition, self-assembly and genetic engineering provide ways to control and manipulate large molecules and ensembles of such molecules. Indeed, recent research was directed towards self-assembled monolayers and thin films of biomolecules as parts of biosensors, protein-based photonic devices, and, even more challenging, electronic current-carrying devices.

Among the proteins that are explored in BME,[1–10] considerable attention has been devoted to bacteriorhodopsin (bR), a light-driven cross-membrane proton pump. The potential of bR for biological device applications stems from its stability towards thermal, chemical, and photochemical degradation, combined with its desirable photoelectric and photochromic properties. Furthermore, both the structure–function relations of bR, and ways to modify bR structure and thus, its functions, have been studied intensively.

However, there are at least two problems associated with integrating bR in a practical system:

- Its structure has to be amenable to integration and
- The interface of bR with the rest of the system has to be optimized for the intended device function. For example, the photoelectric conversion efficiency of a bR film depends strongly on the degree of orientation of the bR protein.[11] Therefore, protein orientation is of major significance and one strives to have bR oriented in the device structure.

However, if bR must also function as an active, current-carrying component, this imposes additional challenges. Thus, for a potentially practical device structure, many bR units are needed, *i.e*., a bR layer with at least μm lateral dimensions. Such a layer must have a pinhole density that is sufficiently low, not only to prevent junction shorting,

[a] *Department of Organic Chemistry, The Weizmann Institute of Science, Rehovot 76100, Israel. E-mail: ydjin1018@yahoo.com.cn. E-mail: mudi.sheves@weizmann.ac.il*
[b] *Department of Materials & Interfaces, The Weizmann Institute of Science, Rehovot 76100, Israel. E-mail: david.cahen@weizmann.ac.il*

Yongdong Jin (PhD with Shaojun Dong from Changchun Inst. of Appl. Chem., Chinese Acad. of Sciences, P. R. China), researched this review's topic as a postdoc with Cahen & Sheves. He currently works in the Dept. of Bioengn., UW-Seattle (with Xiaohu Gao) on bio-/nano interfaces.

Izhar Ron (BSc in Biology, MSc in Biomedical Engn., Tel-Aviv Univ.) does his PhD research, and Tal Honig (BSc, Chemistry HU) did her MSc research with Cahen & Sheves on this review's topic. Noga Friedman (BSc and MSc in chemistry at HU, PhD WIS, postdoc at Univ. of Copenhagen) has been at the WIS since 1974. After a sabbatical at the UCSD, she joined Sheves' group, where she studies the chemistry and biophysics of retinal proteins.

Mordechai Sheves (BSc in chemistry at Bar-Ilan Univ., PhD at the Weizmann Inst. of Science, WIS, postdoc in rhodopsin chemistry at Columbia Univ.), joined the WIS working on the mechanism underlying the function of retinal proteins. His work includes synthesis of retinal analogs, used for preparing artificial pigments of various retinal proteins, biophysics of these proteins and the molecular mechanism underlying their light-induced activation.

David Cahen (BSc in chemistry & physics at the Hebrew Univ., Jerusalem, HU, PhD in materials chemistry at Northwestern Univ. and postdoc in photosynthesis at HU and WIS, joined the WIS, working on solar cells, which he researches also today. These interests led to work on hybrid molecular/non-molecular materials, and on understanding how (bio)molecules can serve as electronic current carriers, and what are the limitations and possibilities for fundamentally novel science with them.

but also partial shorting; otherwise such junctions will not have reliable and reproducible current–voltage (*I–V*) characteristics.

Various physical and especially optical applications of bR have been explored and also reviewed in the past.[4,12–15] Here, we focus on studies that consider bR as an electronic material, particularly as a conduction medium, and we will also review some recent developments. The idea is both to describe the state of the art and provide a perspective of this area in the future, as part of (bio)molecular electronics. We emphasize especially approaches that can lead to interfacing bR with solid electrodes in prototypical current-carrying solid-state structures.

For the integration of functional bR molecules in current-carrying solid-state devices, the following issues will be considered and discussed in this review:

(1) Can electronic current pass through bR in a solid-state (dry) configuration? Measuring any current flow through an ~5 nm-thick membrane, where the protein is embedded, is remarkable, because 5 nm is well beyond the thickness over which tunnelling through an insulator is expected to be efficient, more so if compared to systems with a transport gap, similar to the one estimated for bR (see below, *cf*. ref. 52).

(2) If current passes, what can be the possible mechanism(s)?

(3) Does bR retain its photochemical activity, *i.e*., will any bR photoactivity affect the electronic currents passing through it and will it generate a light-induced photovoltage, following integration into a solid-state device structure?

(4) Is the orientation of bR important for electronic current transport? Does light-driven proton pump activity, or light-induced proton release of bR contribute to the measured junction currents?

2. Structure and biological function of bR

Bacteriorhodopsin (bR) is the sole protein (MW 26 000) found in the purple membrane (PM) of the archaeum *Halobacterium salinarum*.[16] PM consists of a 75% bR and 25% lipid bilayer; it is organized in a two-dimensional (2D) hexagonal crystal lattice with a unit cell dimension of ~6.2 nm. The PM is usually called the bR membrane. Electron crystallography indicates that bR is organized in trimers with lipids mediating the inter-trimer contacts.[17] The extreme brine and high temperature growth conditions of the archaea, together with the hexagonal 2D crystalline lattice structure, give bR exceptional stability to salt, high temperatures, photochemical degradation, chemicals, and extreme pH.[18]

The bR protein consists of 248 amino acids, arranged in seven α-helical bundles inside the lipid membrane, forming a cage, which hosts a retinylidene chromophore, attached to lysine 216 *via* a protonated Schiff base linkage. The retinylidene moiety plays an important role in electron transport (ET) through the protein, as will be shown below. A molecular model of the bR protein is shown in Fig. 1.

bR serves as a light-driven pump, which moves protons from the cytoplasmic (CP) to the extracellular (EC) side of the membrane, thereby generating a substantial electrochemical gradient that is used to synthesize ATP, following the chemiosmotic model.[19] After light absorption, bR converts to a light-adapted state, with the retinal chromophore in the all-*trans* configuration.[20] Light absorption by this form

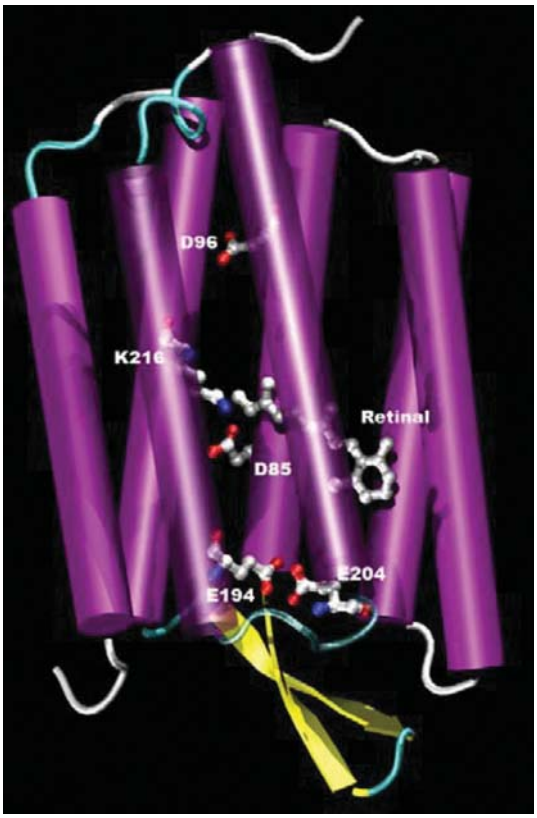

Fig. 1 Schematic representation of the three-dimensional structure of bR. The seven α-helical domains form a transmembrane pore. The retinylidene residue is linked to the protein moiety, *via* a protonated Schiff base linkage to lysine 216. The proton pathway is shown and, in particular, the positions of the aspartic acids 85 and 96 (D85; D96), which act as proton acceptor and donor for the reversible deprotonation and protonation of the Schiff base linkage during the photocycle.

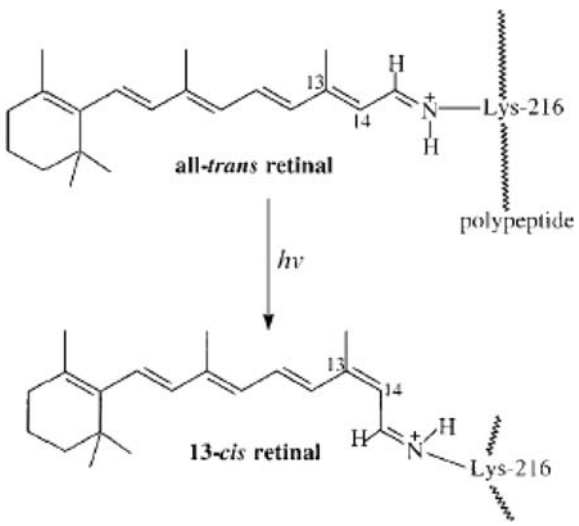

Fig. 2 Photoisomerization of all-*trans* to 13-*cis* retinal in bR. Under illumination by visible light, all-*trans* retinal in light-adapted bR is isomerized to the 13-*cis* conformation around the C_{13}–C_{14} bond, initiating the photocycle of bR.

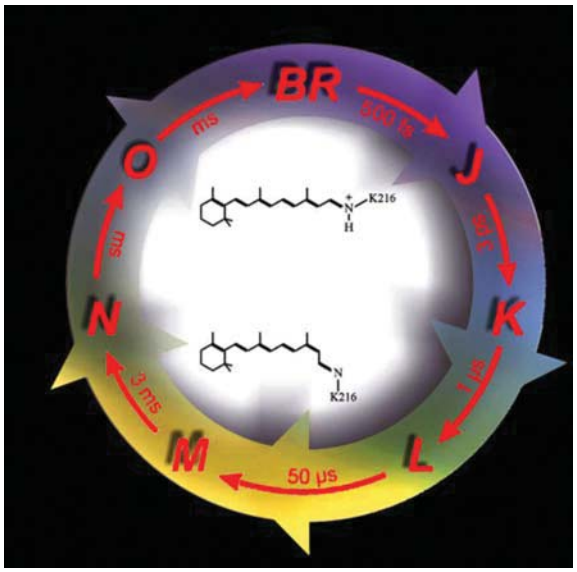

Fig. 3 Schematic of the bR photocycle. The proton transport is initialized by photon absorption and charge separation on the picosecond time scale. After about 50 µs, deprotonation of the Schiff base leads to the M intermediate. In the natural membrane, the photocycle and the proton transport process are completed in 10 ms.

(with a 568 nm absorption maximum) triggers isomerization of the all-*trans* configuration to the 13-*cis* isomer (see Fig. 2). This event initiates the photocycle of bR, shown schematically in Fig. 3, a sequence of transitions through intermediate states, with different spectral absorption properties.[21,22]

The light-driven proton transport process, which occurs on 10^{-12} to 10^{-2} s time scales,[15] is initiated by absorption of green light ($h\nu \approx 560$ nm), followed by an immediate charge separation step. The charge transport through the molecule is associated with de- and re-protonation steps of the retinal Schiff base linkage.

3. Interfacing bR with solid-state electrodes

The first and most important concern on interfacing biological systems with solid support for device applications is to ensure that immobilization onto a solid support does not affect the biological function of interest. bR was reported to maintain its biological activity, if immobilized on solid support[23] and if incorporated in multilayer structures of self-assembled, ordered films. This stability was maintained up to temperatures as high as 140 °C.[18] Our physical characterizations, including photoelectric measurements, indicate that bR monolayers formed by electrostatic interactions retain their photoactivity at ambient (Rehovot) humidity, *i.e.*, ~60% RH (relative humidity).[24–26]

To date, the proposed technical applications of bR can be grouped into four general categories, based on the physiological functions and properties utilized. These are optoelectronics, energy conversion, optical storage & information processing, and nonlinear optics.[27] Each of these bR applications differs in the complexity of the device structures and the demands that these put on the biological components.[15]

The use of bR ***mono***layers for electronic transport studies has the advantage that the structure of bR in the layer is better defined than in ***multi***layers. Therefore, electrical measurements should be more reproducible and the results more amenable to analyses. Thus, finding ways to use bR-containing monolayers in photoelectric device structures to study current transport represents an important basic and applied scientific goal. However, as noted in the introduction, producing high-quality bR monolayers with good orientation and high surface coverage represents a technical challenge. Moreover, if bR monolayers are to be incorporated into solid-state junctions, we need to consider that the current flowing through the junctions can consist of two parts, the net electronic junction current in which bR, like other molecules, acts as an electronic conduction medium (resistance) and a (nominal) Faradaic proton current. The latter arises from the proton pumping ability of bR. This and other complications call for systematic, well-designed experiments and comparisons with calculations to help elucidate how electronic charge carriers flow across bR monolayers.

4. Immobilization, orientation and photoelectrical responses of bR thin films

The most demanding bR-based photoelectric device structure uses the unidirectional, *photocycle-related* electric response. Such a response can be obtained only if bR in the device has a net orientation.[11] Efforts to achieve such orientation have been based, so far, on methods such as Langmuir–Blodgett (LB) deposition, electric field sedimentation (EFS), chemisorption-driven self-assembly, electrostatic layer-by-layer adsorption and antigen–antibody molecular recognition.[27] (Dis)advantages of the various methods have been discussed briefly elsewhere.[26–28] bR monolayer orientation can be improved significantly by electrostatic adsorption using vesicle fusion tactics[24,28] or upon acetylation of the bR lysines.[26] Usually bR orientation has been estimated, based only on the direction and intensity of the photoelectric response of the device, without directly proving the actual orientation of membrane units. This indirect approach frequently leads to confusing or contradictory conclusions.[13]

Wet electrochemical results

A number of electrochemical studies were devoted to the optoelectronic characteristics of bR multilayers, mostly concerning their photovoltage (*cf.* ref. 27), but a few also discussed photocurrents through multilayers (*cf.* ref. 37). In several cases, the results from such samples are relevant for solid-state metal–bR monolayer–metal planar junctions, the topic that we will focus on later.

Work of Koyama *et al.* dealt with the electrical response of monolayers in an aqueous environment.[11,23,29] More specifically, they fabricated a photo-electrochemical cell, where a thin bR film, down to a monolayer, was immobilized at the interface of a transparent conductive electrode and an aqueous electrolyte gel. Upon illumination, this cell produced a characteristic *transient* photocurrent. In Fig. 4, we compare the *transient* photocurrent signals, obtained with the two types of antibody-mediated, bR monolayers. The strongest response

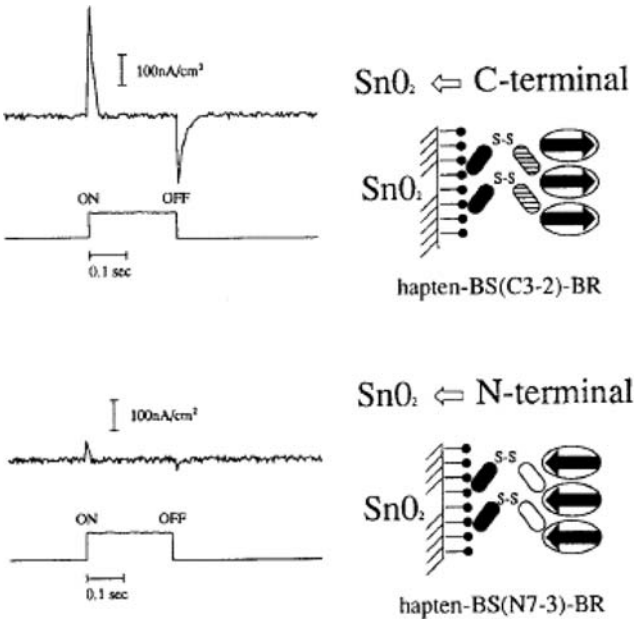

Fig. 4 Comparison of typical photoelectric response from wet sandwich-type photocell. Top: photoelectric response from an oriented monolayer bR film with the cytoplasmic side facing the SnO_2 electrode. Bottom: photoelectric response from an oriented monolayer bR film with the extracellular side facing the SnO_2 electrode. The bR monolayer film was irradiated with green light from a 150 W Xe arc lamp through a filter system that gave an incident intensity of about 10 mW cm^{-2}. The arrows indicate the orientation of bR along the direction of proton pumping. (*Adapted from* ref. 29; *copyright 1995 Wiley-VCH Verlag GmbH & Co.*; *reproduced with permission*).

occurs in the sample with the cytoplasmic (carboxyl terminus) side of bR directed towards the electrode (SnO_2). No measurable *stationary* currents were observed; this was ascribed to the capacitive nature of the underlying SnO_2 electrode.[30]

Recently Horn and Steinem[30] described a new membrane model in which bR was adsorbed on free-standing lipid bilayers, termed nano-black lipid membrane, spanning the holes of porous alumina substrates, with average pore diameters of 280 nm (Fig. 5A). This membrane system exhibits very good long-term stability toward continuous illumination, with the added feature that not only *transient* but also *stationary* currents can be recorded. A typical current trace is given in Fig. 5B.

Photovoltaic results

The photo*voltaic* behavior of bR was studied in films electrodeposited on conductive electrodes.[31–33] Such bR films produce a steady-state photovoltage, accompanied by an initial transient. The photovoltage and the concomitant photocurrent, both of which are normally very small, originate from charge displacement in the bR complex, initiated by photo-isomerization of the retinal chromophore.[23] The photoelectric response time of bR can be as short as 10^{-11} s,[33] if direct contact between the bR membranes and the underlying electrode is achieved. However, the photoelectric behavior of bR films, in contact with electrodes, is affected significantly by the presence of water or ambient humidity,[31,32] reflecting the

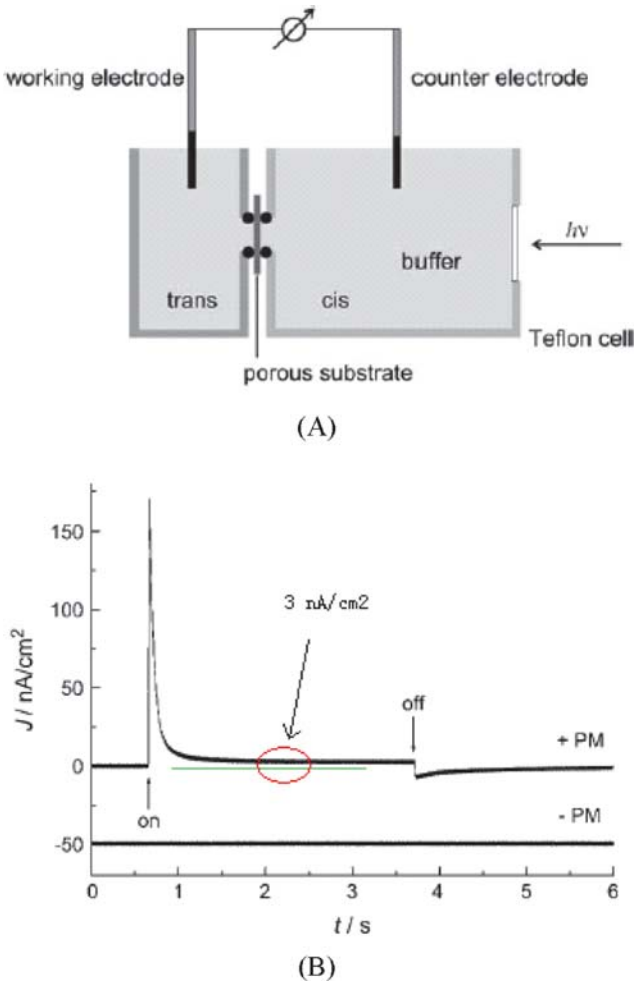

Fig. 5 (A) Experimental setup for measurements with nano-black lipid membrane. Two Teflon half-cells with a porous alumina substrate clamped in between were used for impedance analysis and photocurrent measurements. Electrical contact was achieved by platinized Pt electrodes in both cuvettes. (B) Photocurrent before (−PM) and after (+PM) addition of bR to the *cis* compartment. (+PM): the first transient corresponds to switching the light on, and the second transient corresponds to switching the light off. The current was recorded 40 min after bR addition. (−PM): the current trace corresponds to the signal recorded before addition of purple membranes. No significant photoeffect could be detected. For clarity, the current trace is shifted by −50 nA cm^{-2}. (*Adapted from* ref. 30; *copyright 2005 by the Biophysical Society*; *reproduced with permission*).

direct effect of water on the photocycle and on light-induced charge redistribution in bR.

Dry photoelectric results

Although most electrical measurements of bR were done in an aqueous environment, there are some examples of electrical (photo-voltage/-current) measurements of bR monolayers/multilayers carried out with only strongly bound water present.[24–26,34–41]

Table 1 summarizes the relevant results from a partial literature survey on this aspect. Although there are some differences in bR film preparations, device configurations and experimental conditions, the photovoltage values are

Table 1 Comparison of monolayer-level photo-voltage or -current responses of non-aqueous (dry) bR, deduced from the results of bR monolayers or multilayers performed in different device configurations

Circuit (open/closed)	Film	Biased	Light trigger	Photovoltage, PV (photocurrent, I_{ph})[a]	Ref.
Al/bR/–/Au[c] (open)	Sub-ML[d]	Yes	CW $\lambda > 530$ nm 28 mW cm^{-2}	$\sim$10 mV ML^{-1} (No I_{ph} [e])	25
Al/bR/–/Au (open)	Sub-ML	Yes	CW $\lambda > 530$ nm 28 mW cm^{-2}	$\sim$4 mV ML^{-1} (No I_{ph})	26
ITO/bR/Al (closed)	$\sim$1 μm OF[f]	No	Xenon arc lamp $\sim$1 mW cm^{-2}	No PV[g] ($\sim$3 pA cm^{-2} ML^{-1})	34
ITO/bR/–/Au (open)	4 μm OF	Yes	CW $\lambda = 635$ nm 2 mW cm^{-2}	$\sim$3 mV ML^{-1} (No I_{ph})	35
ITO/bR/–/BGO/ITO[h] (open)	10 μm OF	No	CW $\lambda = 532$ nm 500 μJ cm^{-2}	No PV (No I_{ph})	36
(gate of) GaAs FET (open)	100 μm OF	Yes	CW He-Ne laser 50 μJ cm^{-2}	No PV ($\sim$100 nA ML^{-1})	37
Al/bR/Au (closed)	ML	Yes	CW $\lambda > 530$ nm 28 μJ cm^{-2}	No PV (No I_{ph})	24
ITO/bR/Al (closed)	0.5 μm OF (in polymer)	Yes	CW $\lambda = 532$ nm 2 mW cm^{-2} + chopped $\lambda = 350$–600 nm	No PV ($\sim$40 pA cm^{-2} ML^{-1}) steady-state value	38
ITO/bR/Cu[b] (closed)	PVA[i] sol–gel ($\sim$100 μm)	Yes	Square wave of $\lambda = 532$ nm at 600 mW cm^{-2}	$\sim$0.2 mV ML^{-1} at 20 V external bias ($\sim$6 nA cm^{-2} ML^{-1})	39
ITO/bR/Al (closed)	0.5 μm OF (with polymer)	Yes	CW pump source 2 mW cm^{-2}, $\lambda = 405$ nm	($\sim$40 pA cm^{-2} ML^{-1}) steady-state value	43
ITO/bR/Au/GaAs (closed)	PVA ($\sim$100 μm)	Yes	Laser, $\lambda = 632$ nm 800 mW cm^{-2}	($\sim$0.2 pA cm^{-2} ML^{-1}) steady-state value	44
ITO/AM/bR/AM/InGa[j]	LBL[k]	No	Laser, $\lambda = 532$ nm	$\sim$ 15 mV ML^{-1} (No I_{ph})	42

[a] The values given are those calculated per monolayer, assuming that the photo-voltage/-current response of bR is linearly proportional to the number of bR monolayers, *i.e.*, the data are normalized in terms of the bR content in the multilayers. [b] Measurement taken under an external bias of 20 V. [c] /–/ = A gap in the circuit—open circuit measurement. [d] ML = monolayer. [e] I_{ph} = photocurrent. [f] OF = electric sedimentation oriented film. [g] PV = photovoltage. [h] BGO = bismuth germanium oxide. [i] PVA = poly(vinyl alcohol). [j] AM = apomembrane. [k] LBL = layer by layer with PDAC.

below detection limits or are very low, in the range of $\sim$0.2–15 mV ML^{-1}.[25,26,35,39,42]

Photocurrents

Most photocurrent values are 0.2–40 pA cm^{-2} ML^{-1},[34,38,40,41] with two apparent exceptions[37,39] with much higher values. In one case, bR was incorporated into the gate of a GaAs field effect transistor.[37] bR photoactivity was measured through the effect on the transistor's source–drain current, which did not pass through bR. In the other case, the bR microenvironment might be considered to function like a solution: the bR complex was embedded in a poly(vinyl alcohol) (PVA) matrix and acted as a proton transport species.[39] Even then, a 20 V external voltage and 600 mW cm^{-2} light intensity were necessary to obtain this remarkable result. Both cases are quite different from actual photoelectronic charge carrier measurements across bR films.

(Absence of) photovoltage

Interestingly, except for the above-mentioned case,[39] there are no reports of solely illumination-induced voltage generation if the bR film is at both its sides in direct mechanical contact with a solid electrode. At this point, we can only hypothesize to explain this peculiarity:

As shown by contact potential difference (CPD) measurements,[28] light-induced electrical dipole changes in a dry bR ML should translate into illumination-induced changes in the work function difference between the two electrodes. Therefore, a photovoltage should be measured if enough charge carriers are created at the electrode/bR interface. Indeed, for a bR film, sandwiched between two conductive substrates, *but with an insulating* (apomembrane) *layer separating the active layer from the electrodes*, the generated dipole translates into a measured photovoltage.[42]

It is known that the change in protein dipole, created across the membrane as a result of the proton pumping process, is around 40 debye (D),[40] whereas the (change in) protein dipole, induced by the photochemical retinal *trans–cis* isomerisation is 11 D.[41] From the Helmholtz relation, $\Delta\phi = \frac{N\mu}{\varepsilon\varepsilon_0}$, we can calculate that these values correspond to 100 and 27.5 mV, respectively, while the reported photovoltage values are $\sim$0.2–15 mV.[25,26,35,39,42] Therefore, the measured dipole in dry samples is more likely to originate from the retinal isomerisation than from the proton release. This is reasonable, taking into account that in dry systems the proton sources are limited.

If we calculate the net charge separation across the membrane, 40 D corresponds to 2×10^{-3} electrons, separated by the bR membrane (1 D $\approx 3.3 \times 10^{-28}$ C cm). Separation of 1 electron across the bR membrane would result in a physically unreasonably high dipole moment, or in complete actual charge separation, Such a situation, which is closer to what might be expected for thylakoid membranes, would lead to a much higher trans-membrane voltage difference than the observed one. This discrepancy shows that complete charge separation across the purple membrane is unlikely.

Since experiments show that the membrane is not completely insulating, we speculate that no photovoltage is measured in monolayers due to discharge of the photo-induced dipole through the protein. In the case of bR multilayers or if only one membrane side is in direct mechanical contact with a metallic electrode, such discharge is unlikely, and a more plausible hypothesis is that depolarization occurs at the interface due to the close contact with high electronic carrier density materials.

Similar to what is reported for samples in solution, most photocurrent responses reported for bR film systems are

transient (differential) ones, which disappear within $\sim$1 s upon continuous illumination. However, a few cases of a *steady-state* photocurrent were reported, following a somewhat higher initial peak response of bR in the presence of a conducting polymer[38,43] or in a PVA matrix.[44] The observed steady-state photocurrents are at the pA level ($\sim$0.2–40 pA cm^{-2} ML^{-1}). These values are comparable to the steady-state photocurrent, associated with proton transport, of a bR monolayer ($\sim$0.6 pA ML^{-1}; contact area unknown[45]). That result was obtained from solution-phase cyclic *I–V* dependencies of a bR monolayer, incorporated in a planar bilayer lipid membrane, under both dark and light conditions.[45]

In a hybrid bR/quantum dots (QDs) bio-nanosystem of thin films, prepared by electrophoretic sedimentation (of unspecified thickness), QDs play the role of a secondary, *in situ* nanoscale light source.[46] With the assistance of the QDs' fluorescence, single wavelength blue light illumination was found to induce an $\sim$40 nA cm^{-2} *stationary* photocurrent through the films.

5. Current transport through bR in a solid-state structure

Although bR is an interesting test case for biomolecular electronics, systematic ET studies through bR are hampered by the difficulty of finding a reliable, reproducible experimental system that allows such measurements.

5.1 Current transport through bR, as revealed by using STM for imaging

When electronic current flow was first measured across dry, solid-supported bR, the membrane was used more as a model system to examine the conditions for reproducible scanning tunnelling microscope (STM) imaging of biological specimens than for studying ET across it.[47–50] STM, operated in the field emission regime ($>$5.5 V applied voltage), and at very low current set-points ($\leq$2 pA), can generate high-resolution images of hydrated bR and the sample is modified by increasing the current.[48,49] Contrast reversal was observed, which was explained by a model, based on field emission and on the presence of empty electronic states in the proteins. In general, there is still an ongoing discussion regarding STM experiments on biomolecules, both theoretical and experimental. In light of the extreme conditions used for this STM imaging, direct tunnelling through the biomolecules is thought to contribute negligibly to the total current. As for bR, it was proposed that electron field-emission from sites on the molecules led to conduction enhancement and that the observed contrast reversal was related to the lateral conductivity of water films present in the hydrated samples used.[50]

Although the actual ET mechanisms, involved in the STM experiments with several nm-thick macromolecules (like bR here) are not known, our recent finding of current transport through supposedly insulating layers that are 5 nm thick, because of enhancement by gold nanoparticles,[51] suggests that conduction in the STM experiments may be related to the nm-sized apex of the STM tip.

5.2 Current transport through bR—conducting probe AFM studies

Conducting probe AFM (CP-AFM) offers an approach that is more compatible for studying current transport across biological molecules. The main features it introduces, which differ from STM, are (1) direct mechanical contact between the electrode (tip) and sample, (2) tight feedback on the exerted

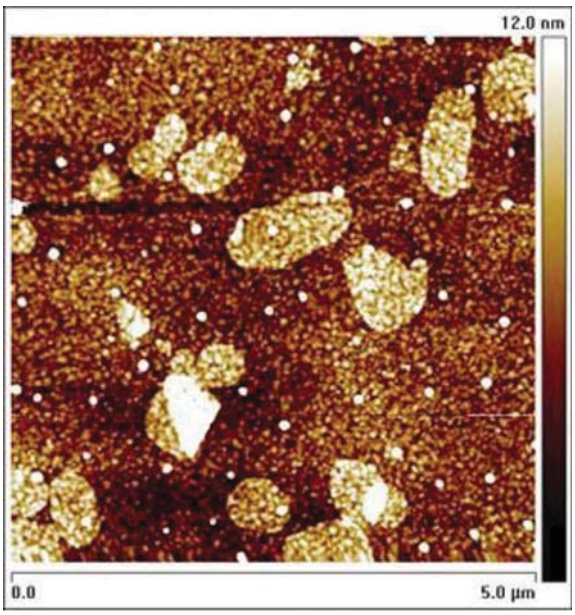

(a)

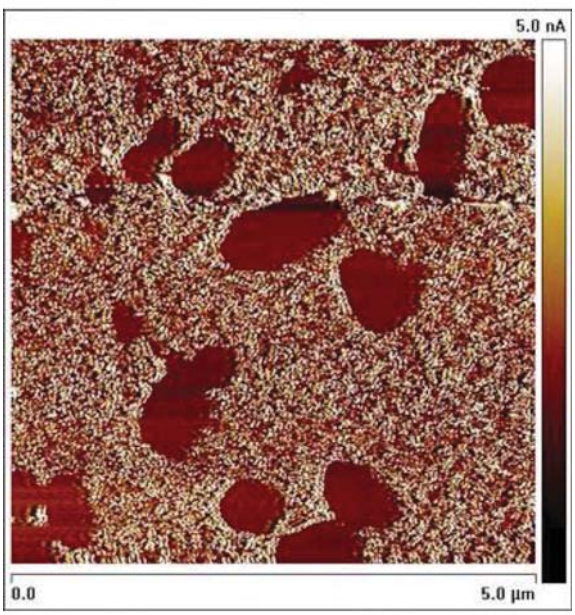

(b)

Fig. 6 AFM topography (a) and current (b) images of wild-type bR-containing membranes, deposited on a bare Au substrate. Images were taken with a Nanoscope III multimode instrument (DI, Veeco technologies, Inc.) under ambient conditions, using a Pt/Ir-coated tip (Nanosensors) under a constant bias voltage of 2 V.

force and (3) ability to monitor continuously the morphology of the sample, regardless of the measured electrical signals. We carried out such studies in the past to determine whether measuring current through a single bR trimer is possible. A scan in contact mode under fixed bias voltage revealed that if current does flow, its magnitude is below the detection limit of the measuring system. This can be seen by zeroing the current signal wherever the tip scans a 5 nm-high membrane patch (Fig. 6). CP-AFM also allows positioning of the tip over a chosen point in the image and recording *I–V* curves. However, measurements are not stable with this approach.

Similar results of AFM scans under bias voltage were reported, but, additionally, *I–V* curves were recorded over selected membrane fragments. Those measurements were reported to be reproducible, possibly because of the very high applied potentials.[52] In both cases, CP-AFM seems limited, at least for bR, by the low signals that one tries to measure. Thus, future work may require significantly larger area AFM tips to carry out investigations at more reasonably applied voltages.

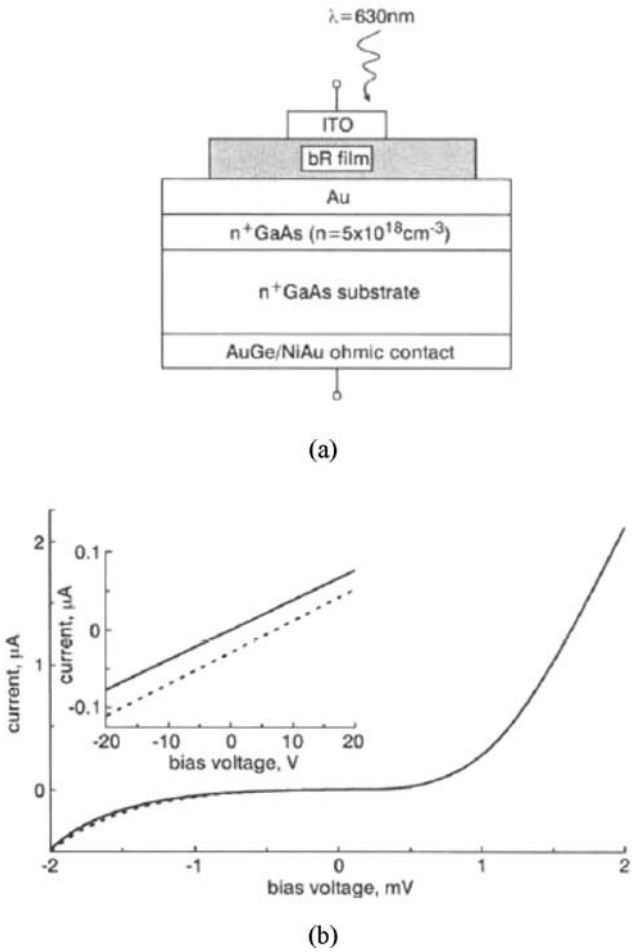

Fig. 7 (a) Schematic diagram of an ITO/bR/Au/GaAs heterostructure for measuring photoconduction across the bR sample; (b) Current–voltage characteristics measured in the dark and under illumination (λ = 630 nm): — dark; - - - laser illumination (100 mW mm^{-2}). Inset: zoom-in near-zero bias. (*Adapted from* ref. 44; *copyright 2001 IEEE*; *reproduced with permission*).

Macroscopic *I–V* measurements on (sub)monolayers, prepared from native bR patches, failed owing to the inability to control the occurrence of short-circuiting, *i.e.*, reproducibility was affected by the existence of uncontrolled current paths in the incomplete monolayer. These practical issues led to a situation where, to date, there have been only a few reports on bR monolayers, mostly preliminary ones on current flow through bR multilayers[44] and bR patches[47–50] in dry systems.

5.3 Current transport through bR multilayer heterostructures

Xu *et al.*[44] reported transient and steady-state photoconduction across an indium tin oxide (ITO)/bR/Au/GaAs heterostructure, with bR acting as the light-sensitive material. The hybrid semiconductor–Au–bR heterostructure is schematically shown in Fig. 7a. The thickness of the bR layer, which is randomly oriented in a PVA matrix, is ~100 μm and the Au layer is thick enough to ensure that the light, transmitted through it into the GaAs, is negligible, so as to exclude any GaAs photoeffects. The steady-state *I–V* characteristics of the device in the dark and under illumination are shown in Fig. 7b. They are similar to those of a Au–GaAs Schottky diode, with added series resistance of the bR layer and ITO contact. If we assume that the current is distributed homogeneously, *e.g.*, if it flows through the bR molecules, then we can obtain a short-circuit photocurrent of ~8 pA cm^{-2} ML^{-1}. The steady-state photoconduction may be due to the pH change at the bR/ITO interface, as a result of protons released from the bR–PVA multilayer film upon photo-excitation.[44] The rather poor definition of the interfaces in these measurements precluded

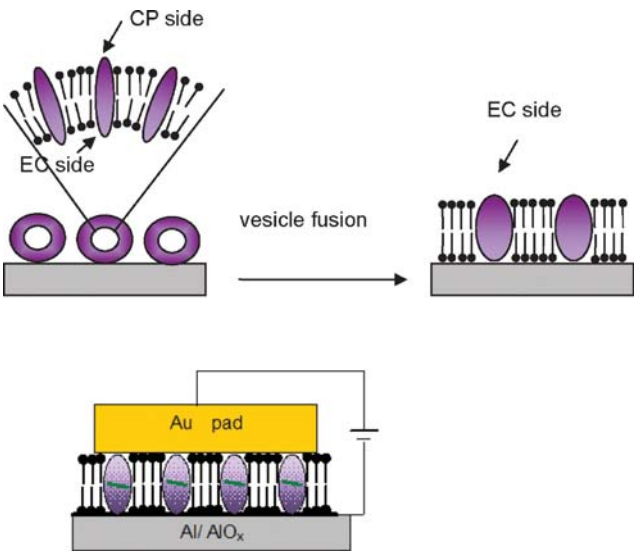

Fig. 8 (Top) Schematic presentation of monolayer formation of oriented bR membranes. The inside-out orientation of the bR protein in vesicles dictates that, after vesicle fusion, the bR in the monolayer is oriented with its cytoplasmic side facing the substrate. (Bottom) Schematic planar junction configuration used for electronic current transport measurements. bR, with a retinal in the central region, is incorporated in the fused lipid bilayers as a separate component of the array, with the cytoplasmic (CP) and extracellular (EC) sides vertical to the contact surfaces. (*Adapted from* ref. 28; *copyright 2007 Wiley-VCH Verlag GmbH & Co.*; *reproduced with permission*).

a systematic study of the underlying mechanisms involved in the current transport.

5.4 Current transport through planar metal–bR monolayer–metal junctions

Reconstituting bR in lipid bilayers on a solid, electrically conducting support *via* vesicle fusion tactics[53] is a convenient approach for systematic electronic transport measurements of bR in monolayer form.[24,28] This method is based on top (electrical) contact deposition, using the 'lift-off, float-on' (LOFO) method, where a 'ready-made' metal patch is used as top contact.[54] Fig. 8 shows schematically the vesicle fusion tactics, and also the junction configuration used in these studies. Monolayers of native membranes, of apomembranes (*i.e.*, with retinaloxime or without retinaloxime), and of

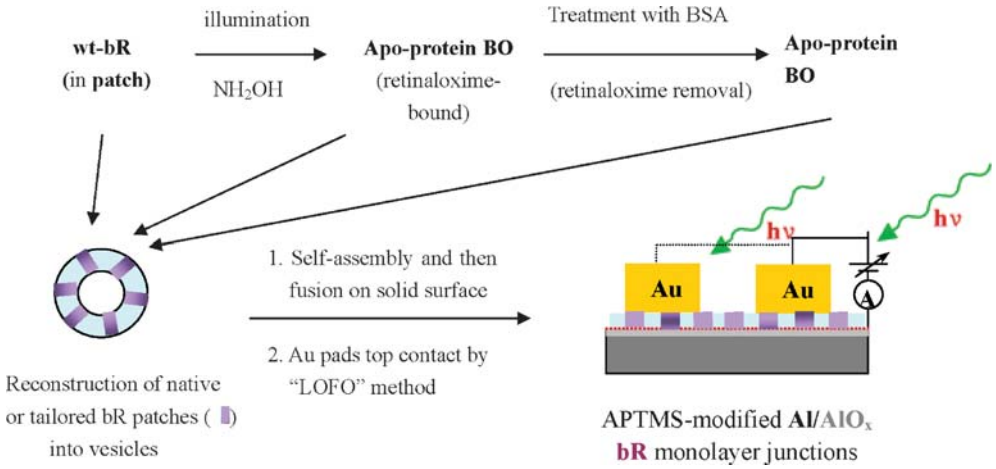

Fig. 9 Scheme for preparing artificial bR-containing membranes and their reconstruction into vesicles, preparation of the metal–protein–metal junction and the measuring scheme. (*Adapted from* ref. 24; *copyright (2006) National Academy of Sciences, USA*; *reproduced with permission*).

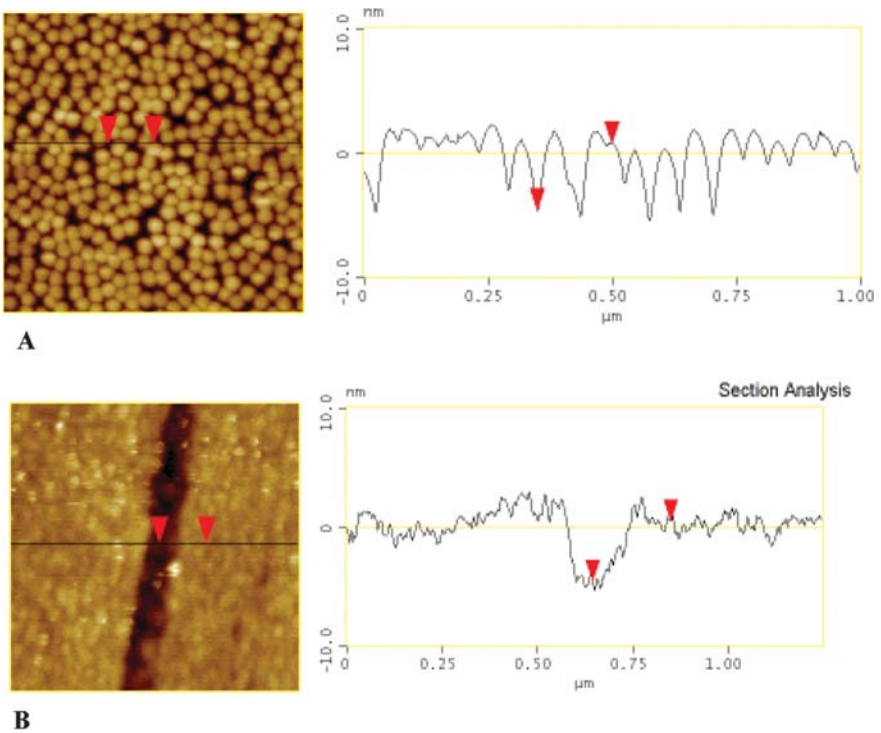

Fig. 10 (A) AFM images (1 µm edge lengths) of monolayers of fused membranes of bR-containing vesicles, prepared by 10 min adsorption of bR–PC vesicles on Al/AlO_x substrate, derivatized with APTMS ((3-aminopropyl)trimethoxysilane). The line scan shows an average height of the strongest features of ~5.4 nm. The height bar covers 20 nm. (*Adapted from* ref. 28; *copyright 2007 Wiley-VCH Verlag GmbH & Co.*; *reproduced with permission*). (B) A more densely packed bR-containing monolayer, prepared by 20 min adsorption of vesicles on the substrate (1.25 × 1.25 µm image). The crack in the membrane, induced by excessive drying, shows the monolayer to be 5.1 nm thick (between markers). (*Adapted from* ref. 24; *copyright (2006) National Academy of Sciences, USA*; *reproduced with permission*).

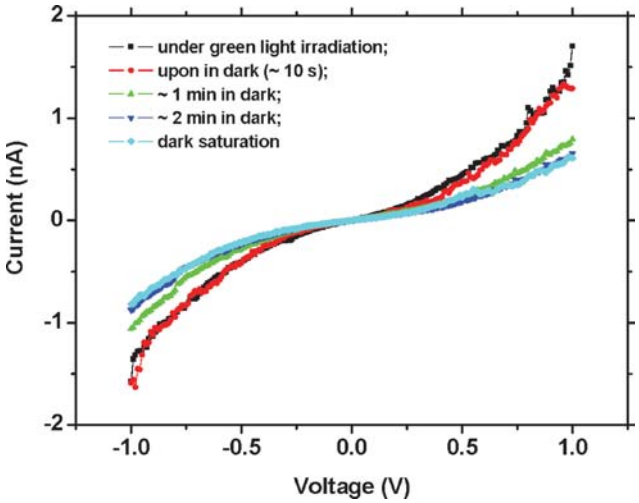

Fig. 11 Time evolution of *I–V* curves of the Au/bR/APTMS–AlO_x–Al junction, containing an oriented bR monolayer prepared by bR–PC vesicle fusion, measured under ambient conditions, in the dark, upon $\lambda > 550$ nm illumination and dark adaptation. Optically measured geometric Au pad area: 2×10^{-3} cm^2. (*Adapted from* ref. 28; *copyright 2007 Wiley-VCH Verlag GmbH & Co.*; *reproduced with permission*).

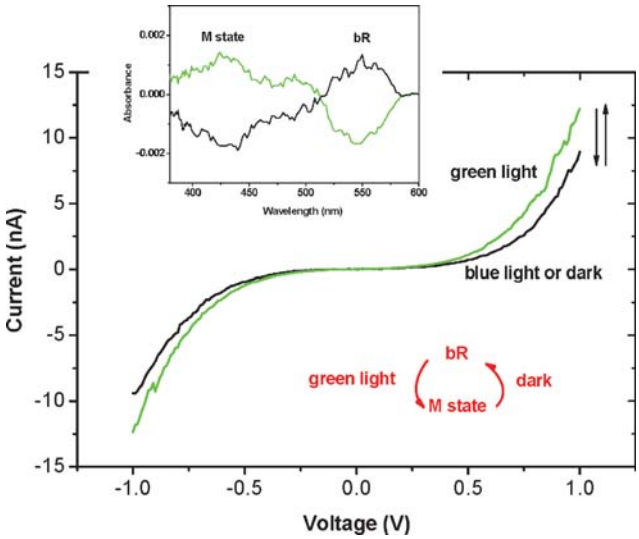

Fig. 12 Current–voltage (*I–V*) curves of Au/bR/APTMS–AlO_x–Al junction, with an oriented bR monolayer, prepared by bR–OTG vesicle fusion, measured under ambient conditions, in the dark, upon $\lambda > 550$ nm illumination and upon illumination with (380 nm $< \lambda <$ 440 nm) light. The arrows show that the *I–V* responses can be cycled by switching between the two types of illumination. Au pad area: 2×10^{-3} cm^2. Inset: absorption difference spectra of two bR monolayers, adsorbed on each side of an APTMS-modified quartz slide, as a result of green light irradiation and dark adaptation. Green curve: irradiated–dark; black curve: (dark after illumination)–irradiated. (*Adapted from* ref. 28; *copyright 2007 Wiley-VCH Verlag GmbH & Co.*; *reproduced with permission*).

membranes with artificial bR pigments, derived from synthetic retinal analogues, were studied. The experimental diagram is shown schematically in Fig. 9.

Fig. 10 shows representative AFM images of a substrate, covered by bR-containing fused PC (phosphatidylcholine) vesicle membranes, prepared by 10–20 min electrostatic adsorption on the substrate. The AFM images show that the membrane coverage is high (>90%), with some sample-free cracks or pinholes (typical tens of nm) between fused vesicle membranes. These are small enough to be spanned by the 'ready-made' Au pads, thus allowing macroscopic transport measurements. Section analysis, from cracks or pinholes, reveals the highest average height feature to be ~5 nm, in good agreement with the thickness of a single bR patch and a PC bilayer. This is thus indicative of a monolayer, 1 bR patch thick, embedded in a PC bilayer.

Fig. 11 shows *I–V* characteristics at 293 K and 40% RH of the planar junction structures shown in Fig. 8 and 9. These *I–V* curves were recorded after dark equilibration, followed by irradiation with green light ($\lambda > 550$ nm; 20 mW cm^{-2}). The dark equilibrated samples passed ~0.6 nA current at 1 V applied bias (300 nA cm^{-2}). Illumination with green light increased the current at 1 V applied bias from 0.6 to 1.7 nA. The system can be cycled between these two states by alternating green light irradiation and dark adaptation. Following green light illumination, the current thermally decays over 2–3 minutes to its original dark equilibration value. Fig. 11 shows the change in the *I–V* characteristics of such a junction after turning off the green light.

The magnitude of junction currents was found to be linearly proportional to the amount of bR in the monolayer junctions, as confirmed by measuring junctions prepared from octylthioglucoside (OTG) (instead of PC) vesicles, in which the bR content is ~6 times higher than in the PC vesicles. Fig. 12 shows typical *I–V* characteristics of such OTG junctions, which are similar to the PC ones, shown in Fig. 11. In the dark-adapted form (or under blue light illumination), 8.9 nA flows at 1 V applied bias. Sample illumination with green light indicated that the steady-state current increases from 8.9 to 12.1 nA at 1 V bias. This bR content-dependent current characteristic, along with the fact that no current was measured through control samples made with apomembranes (see below), indicates that electrons pass mainly *via* bR, rather than through the lipid bilayers.[24,28] A current of 3×10^{-19} A per bR trimer at 1 V bias was calculated. Comparing this current with simulations of what is estimated for direct tunnelling through 5 nm peptides,[55] alkyls or a dielectric medium with a similar dielectric constant, shows it to be several orders of magnitude higher than expected. It is therefore likely that the process of current transport is not (only) straightforward tunnelling through a single barrier.[24,28] The very small current that we calculate for a single bR trimer explains the earlier mentioned problem of CP-AFM measurements on bR.

None of the experimental *I–V* curves displayed any appreciable photo*voltage* that can be associated with the bR photocycle or proton movement, following light absorption. Although the net orientation of bR was confirmed by CPD measurements,[28] *I–V* curves of bR monolayer junctions, even under green light illumination, are almost symmetric and the current at 0 V is zero (*i.e.*, no detectable photocurrent at zero voltage or photovoltage at zero current), within experimental error (~10 pA). This indicates that any light-driven proton

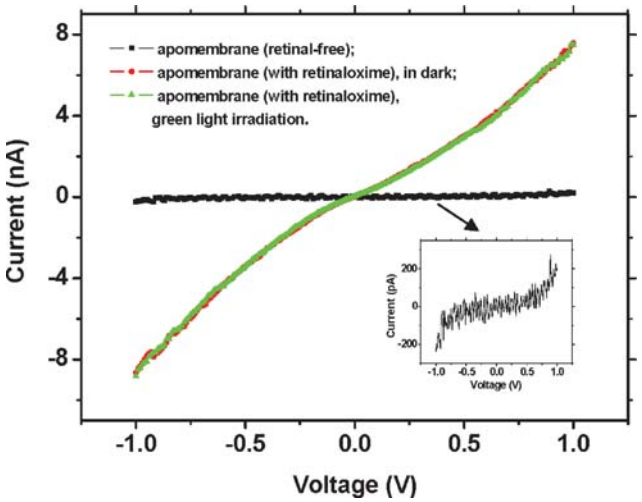

Fig. 13 Current–voltage (*I–V*) characteristics of Au/apomembrane/APTMS–AlO_x–Al junction prepared by vesicle fusion, before and after retinaloxime removal, measured at ambient conditions. There is no detectable photo-effect ($\lambda > 550$ nm illumination) on the junction current of the Au/apomembrane (with retinaloxime)/APTMS–AlO_x–Al junction. (Inset) *I–V* characteristic of the Au/apomembrane (retinal-free)/APTMS–AlO_x–Al junction. Au pad area: 2×10^{-3} cm^2. (*Adapted from* ref. 28; *copyright 2007 Wiley-VCH Verlag GmbH & Co.*; *reproduced with permission*).

pumping that might occur in the sandwiched bR monolayer contributes negligibly to these steady-state photocurrents.[56] Also the experimental data suggest that the green light-induced increase in junction current (from $\sim$0.5 to $\sim$1.5 μA cm^{-2}) cannot be ascribed to the known Faradaic proton current, induced by bR light absorption. This is further confirmed by the reported proton-related photocurrent responses of non-aqueous (dry) bR, calculated for a monolayer, $\sim$0.2–$\sim$40 pA m^{-2} ML^{-1} (Table 1).

The green light-induced increase in junction current appears, from absorption spectroscopy, to be associated with the bR photocycle and its photochemically induced M intermediate. In the junction bR maintained its photoactivity and upon green light illumination (>495 nm), the characteristic ground-state bR absorption, with an $\sim$560 nm maximum, disappeared and a new $\sim$420 nm band appeared, indicating M formation (Fig. 12, insert). The photochemically induced M intermediate thermally decayed to the ground state in a few minutes, as evident by the formation of the 560 nm band and the disappearance of the 420 nm band.[28] Therefore, although it was not possible to find evidence for the complete bR photocycle, clearly irradiation of the junctions produced an M-like intermediate.

No junction photocurrents are generated once the photocycle is blocked or if the retinal cannot isomerize following light absorption. Thus, no detectable photo-effect of currents was observed in junctions derived from apomembranes that contain retinaloxime (Fig. 13). Lack of a photo-effect in junctions made with apomembranes is consistent with the absence of a photocycle in these samples.[57] Moreover, no photo-effect was detected[28] using junctions prepared with artificial pigments inserted into the protein, derived from 13-*cis* (or all-*trans*)-'locked' retinals,[58] in which the critical C_{13}=C_{14} isomerisation is blocked by a 5-membered ring structure.[58]

Measurable currents pass only if the protein contains retinal or an analogue. Current flow through the (retinal-free) apomembrane is orders of magnitude lower than what was observed in native bR membranes and was at noise level (Fig. 13). This result supports the idea that current flows mainly through the bR proteins, that the centrally located retinal serves as current transport mediator and that the photo-effect of native bR-containing membrane junctions can be ascribed to the retinal.

6. Conclusions

We reviewed bR as a medium for biomolecular electronics to provide an experimental perspective in this area of research, emphasizing the issue of interfacing bio-functional bR, especially as a monolayer solid-state electronic device element.

Summarizing we can now answer some of the questions that we asked in section 1:

(1) $\sim 3 \times 10^{-19}$ A per bR trimer (at 1 V bias) electronic current can pass through bR in a solid-state (dry) configuration. Although small, this is > 4 orders of magnitude higher than what can be estimated for direct tunnelling through 5 nm water-free peptides.

(2) The exact current transport mechanism(s) are not known at present, but it seems clear that current transport is mediated by the protein retinal. It is likely that electronic transport benefits from the existence of the path for protons in bR, but the exact current transport paths are not known.

(3) bR retains its functionality, after it is integrated as a monolayer into a solid-state planar junction. The junctions exhibit photoconductivity, and the junction photocurrents are found to be associated with the photochemically induced M-like intermediate of the bR photocycle. However, the light-driven proton pumping activity of the sandwiched bR monolayer, at ambient RH, contributes negligibly to the measured steady-state junction light-currents. These findings, therefore, imply that the electronic features derived from the chemical structure of bR (conductance), rather than the original (proton pumping) function-related chemical properties, are mostly responsible for ET processes in a solid-state configuration.

(4) Although bR orientation is crucial to other optoelectronic device applications, it is not yet clear, whether bR orientation is indeed important for the observed *I–V* characteristics or not, because no photovoltage at zero current (or *vice versa*) is measured.

Acknowledgements

We thank the Ilse Katz Centre for Materials Research (MS, DC), the Helen & Milton A. Kimmelman Center for Biomolecular Structure & Assembly (MS), the Nancy and Stephen Grand Centre for Sensors and Security (DC, YJ, IR), the Gerhard Schmidt Minerva Centre for Supramolecular Architecture (DC, YJ) and the historic generosity of the Perlman family. YJ thanks the Feinberg Graduate School of the Weizmann Institute for a postdoctoral fellowship. MS holds the Katzir-Makineni Chair in Chemistry. DC holds the Rowland and Sylvia Schaefer Chair in Energy Research.

References

1 N. N. Vsevolodov, *Biomolecular electronics. An introduction via photosensitive proteins*, Birkhauser, Boston, 1998.
2 E. Greenbaum, *J. Phys. Chem.*, 1990, **94**, 6151–6153.
3 S. G. Boxer, J. Stocker, S. Franzen and J. Salafsky, in *Molecular electronics: science and technology*, ed. A. Aviram, American Inst. of Physics, NY, 1992, vol. 262, pp. 226–241.
4 R. R. Birge, *Annu. Rev. Phys. Chem.*, 1990, **41**, 683–733.
5 I. Lee, J. W. Lee and E. Greenbaum, *Phys. Rev. Lett.*, 1997, **79**, 3294–3297.
6 L. Frolov, Y. Rosenwarks, C. Carmeli and I. Carmeli, *Adv. Mater.*, 2005, **17**, 2434–2437.
7 G. Maruccio, A. Biasco, P. Visconti, A. Bramanti, P. P. Pompa, F. Calabi, R. Cingolani, R. Rinaldi, S. Corni, R. D. Felice, E. Molinari, M. P. Verbeet and G. W. Canters, *Adv. Mater.*, 2005, **17**, 816–822.
8 Q. J. Chi, O. Farver and J. Ulstrup, *Proc. Natl. Acad. Sci. U. S. A.*, 2005, **102**, 16203–16208.
9 R. Rinaldi, A. Biasco, G. Maruccio, R. Cingolani, D. Alliata, L. Andolfi, P. Facci, F. De Rienzo, R. Di Felice and E. Molinari, *Adv. Mater.*, 2002, **14**, 1453–1457.
10 E. Katz and I. Willner, *Angew. Chem., Int. Ed.*, 2004, **43**, 6042–6108.
11 K. Koyama, N. Yamaguchi and T. Miyasaka, *Science*, 1994, **265**, 762–765.
12 F. T. Hong, *Prog. Surf. Sci.*, 1999, **62**, 1–237.
13 H. W. Trissl, *Photochem. Photobiol.*, 1990, **51**, 793–818.
14 D. Oesterhelt, C. Brauchle and N. Hampp, *Q. Rev. Biophys.*, 1991, **24**, 425–478.
15 N. Hampp, *Chem. Rev.*, 2000, **100**, 1755–1776.
16 W. Stoeckenius, R. H. Lozier and R. A. Bogomoloni, *Biochim. Biophys. Acta*, 1979, **505**, 215–278.
17 R. Henderson and P. N. T. Unwin, *Nature*, 1975, **257**, 28–32.
18 Y. Shen, C. R. Safinya, K. S. Liang, A. F. Ruppert and K. J. Rothschild, *Nature*, 1993, **366**, 48–50.
19 P. Mitchell, *Nature*, 1961, **191**, 144–148.
20 S. P. Balashov, E. S. Imasheva, R. Govindjee, M. Sheves and T. G. Ebrey, *Biophys. J.*, 1996, **71**, 1973–1984.
21 L. Zimányi, G. Váró, M. Chang, B. Ni, R. Needleman and J. K. Lanyi, *Biochemistry*, 1992, **31**, 8535–8543.
22 J. K. Lanyi and G. Váró, *Isr. J. Chem.*, 1995, **35**, 365–385.
23 T. Miyasaka, K. Koyama and I. Itoh, *Science*, 1992, **255**, 342–344.
24 Y. D. Jin, N. Friedman, M. Sheves, T. He and D. Cahen, *Proc. Natl. Acad. Sci. U. S. A.*, 2006, **103**, 8601–8606.
25 T. He, N. Friedman, D. Cahen and M. Sheves, *Adv. Mater.*, 2005, **17**, 1023–1027.
26 Y. D. Jin, N. Friedman, D. Cahen and M. Sheves, *Chem. Commun.*, 2006, 1310–1312.
27 J.-A. He, L. Samuelson, L. Li, J. Kumar and S. K. Tripathy, *Adv. Mater.*, 1999, **11**, 435–446, and related references cited therein.
28 Y. D. Jin, N. Friedman, M. Sheves and D. Cahen, *Adv. Funct. Mater.*, 2007, **17**, 1417–1428.
29 K. Koyama, N. Yamaguchi and T. Miyasaka, *Adv. Mater.*, 1995, **7**, 590–594.
30 C. Horn and C. Steinem, *Biophys. J.*, 2005, **89**, 1046–1054.
31 G. Váró, *Acta Biol. Acad. Sci. Hung.*, 1981, **32**, 301–310.
32 A. A. Kononenko, E. P. Lukashev, S. K. Chamorovsky, A. V. Maximychev, S. F. Timashev, L. N. Chekulaeva, A. B. Rubin and V. Z. Paschenko, *Biochim. Biophys. Acta*, 1987, **892**, 56–67.
33 R. Simmeth and G. W. Rayfield, *Biophys. J.*, 1990, **57**, 1099–1101.
34 J. H. Min, H.-G. Choi, J.-W. Choi, W. H. Lee and U. R. Kim, *Thin Solid Films*, 1998, **327–329**, 698–702.
35 S. Crittenden, S. Howell, R. Reifenberger, J. Hillebrecht and R. R. Birge, *Nanotechnology*, 2003, **14**, 562–565.
36 J. Xu, A. B. Stickrath, P. Bhattacharya, J. Nees, G. Váró, J. R. Hillebrecht, L. Ren and R. R. Birge, *Biophys. J.*, 2003, **85**, 1128–1134.
37 P. Bhattacharya, J. Xu, G. Váró, D. L. Marcy and R. R. Birge, *Opt. Lett.*, 2002, **27**, 839–841.
38 A. G. Manoj and K. S. Narayan, *Appl. Phys. Lett.*, 2003, **83**, 3614–3616.
39 L. M. Zhang, T. Y. Zeng, K. Cooper and R. O. Claus, *Biophys. J.*, 2003, **84**, 2502–2507.
40 A. Lewis, A. Khatchatouriants, M. Treinin, Z. Chen, G. Peleg, N. Friedman, O. Bouevitch, Z. Rothman, L. Loew and M. Sheves, *Chem. Phys.*, 1999, **245**, 133.
41 B. E. Fuller, T. L. Okajima and F. T. Hong, *Bioelectrochem. Bioenerg.*, 1995, **37**, 109.
42 M. Li, B. Li, L. Jiang, T. Tussila, N. Tkachenko and H. Lemmetyinen, *Chem. Lett.*, 2000, **29**, 266.
43 A. G. Manoj and K. S. Narayan, *Biosens. Bioelectron.*, 2004, **19**, 1067–1074.
44 J. Xu, P. Bhattacharya, D. L. Marcy, J. A. Stuart and R. R. Birge, *Electron. Lett.*, 2001, **37**, 648–649.
45 V. I. Portnov, V. M. Mirsky and V. S. Markin, *Bioelectrochem. Bioenerg.*, 1990, **23**, 45–63.
46 R. Li, C. M. Li, H. F. Bao, Q. L. Bao and V. S. Lee, *Appl. Phys. Lett.*, 2007, **91**, 223901.
47 H. E.-M. Niemi, M. Ikonen, J. M. Levlin and H. Lemmetyinen, *Langmuir*, 1993, **9**, 2436–2447.
48 R. García, *Appl. Phys. Lett.*, 1994, **64**, 1162–1164.
49 R. García, J. Tamayo, J. M. Soler and C. Bustamante, *Langmuir*, 1995, **11**, 2109–2114.
50 R. García, J. Tamayo and C. Bustamante, *Int. J. Imaging Syst. Technol.*, 1997, **8**, 168–174.
51 Y. D. Jin, D. Cahen, N. Friedman and M. Sheves, *Angew. Chem., Int. Ed.*, 2006, **45**, 6325–6328.
52 I. Casuso, L. Fumagalli, J. Samitier, E. Padros, L. Reggiani, V. Akimov and G. Gomila, *Nanotechnology*, 2007, **18**, 465503.
53 C. Steinem, A. Janshoff, F. Höhn, M. Sieber and H.-J. Galla, *Chem. Phys. Lipids*, 1997, **89**, 141–152.
54 A. Vilan, A. Shanzer and D. Cahen, *Nature*, 2000, **404**, 166–168.
55 X. Y. Xiao, B. Q. Xu and N. J. Tao, *J. Am. Chem. Soc.*, 2004, **126**, 5370–5371.
56 Upon sample exposure to green light, at 0 V there should be some (proton) current; also an oriented bR monolayer generates a unidirectional photocurrent that should cause a shift in the *I–V* curve (photovoltage at zero current).
57 B. Becher and J. Y. Cassim, *Biophys. J.*, 1977, **19**, 285–297.
58 A. Aharoni, M. Ottolenghi and M. Sheves, *Biophys. J.*, 2002, **82**, 2617–2626.